Experimental Verification of Low-Voltage Power Supply with 10,000-A Pulse Output for Spark Plasma Sintering

Koji Orikawa, Jun-ichi Itoh
Department of Electrical Engineering
Nagaoka University of Technology
Nagaoka, Japan
orikawa@vos.nagaokaut.ac.jp, itoh@vos.nagaokaut.ac.jp

***Abstract*— This paper discusses a high-efficiency power supply developed for implementation under low-voltage and high-current conditions for sintering applications such as the Spark Plasma Sintering (SPS) and so on. The proposed system consists of four 2,500-A units of the power supply connected in parallel. The output voltage of the proposed system is very low because load resistance is usually very small in SPS applications. Therefore, on the output side, many circuit components are connected in parallel. Especially, in the prototype circuit, many schottky barrier diodes are connected in parallel. As a result, equivalent parasitic capacitance of them could not be ignored from the view point of surge voltage. First, the circuit configuration and the control principle for the proposed low-voltage, high-current power supply are described. Second, the influence of the parasitic capacitance of them and parasitic inductances of each snubber component are clarified by theoretical discussion and simulations. Next, the prototype circuit demonstrates that each individual circuit yields a balanced output. Moreover, temperature of each component is measured during long time operation of the prototype circuit. Finally, it is clarified that experimental results of the surge voltage on the schottky barrier diode are correspond to the theoretical discussion by experiments.**

Keywords—AC-DC power converters; snubbers; surge protection

I. INTRODUCTION

The SPS is known as one of sintering techniques that create contacts and bond between particles by heating molded powder material which is ceramic and graphite and so on below their melting point. In this method, the molded powder material is sintered by mechanical pressurization and pulse heating. As a result, the SPS can achieve short sintering time compared to conventional methods such as a pressure less sintering method and a hot pressing method and so on. In this process, the pulse voltage requires a low-voltage and high-current power supply. A thyristor rectifier is well known for it as a conventional circuit [1-5]. However, it has low efficiency and input power factor of approximately 60% and 40%, respectively [5]. On the other hand, power converters using high-speed power semiconductors, such as IGBT and MOSFET, have been proposed for application in sintering power systems in order to improve the efficiency and also reduce the size [5-8]. In Ref [8], a prototype model with an output of 10,000 A has been verified. The prototype model consists of four unit outputs of 2,500 A connected in parallel. The operation characteristics such as the input power factor, the efficiency, and the loss distribution have been evaluated. However, the output current was DC current for fundamental operations even though the SPS actually requires pulse voltage for materials.

Generally, material used in the SPS has a small resistance. Therefore, low voltage is required for the output voltage of power supply. For low output voltage, the transformer which can step down the voltage is used. In addition, the rectifier is connected the output of the transformer. As a result, the surge voltage occurs at the rectifier diode of the secondary side of the transformer [9, 10]. In Ref. [10], only a capacitor which has a small capacitance is connected to the output terminal as a snubber capacitor. This snubber circuit is very simple and low cost. However, adding a capacitor to the output terminal makes the range of the output voltage control narrow. If a phase shift control method is applied, the output voltage is not drastically changed even the phase shift angle is adjusted when the capacitor is connected to the output terminal because the capacitor smoothes the output voltage. Moreover, if the output current is large, a leakage inductance should be lower, and the subber capacitance should be larger. In addition, if a positive output terminal and a negative output terminal are not closed, the snubber capacitor cannot be closer connected. Therefore, the snubber circuit used in Ref [10] is not proper for the SPS which outputs large output current. For the SPS, a snubber circuit which can be closer connected to each rectifier diode is more effective.

This paper verifies a system topology wherein a 10,000-A pulse output current power converter. First, the configuration of the proposed system and control method are introduced. Secondly, the snubber circuit for the rectifier on the secondary side of the transformer is analyzed. Next, an operation of the prototype circuit is experimentally confirmed. As a result, it is confirmed that the prototype circuit can achieve long time operation for the SPS from the experiment which measures the temperature of IGBTs, a

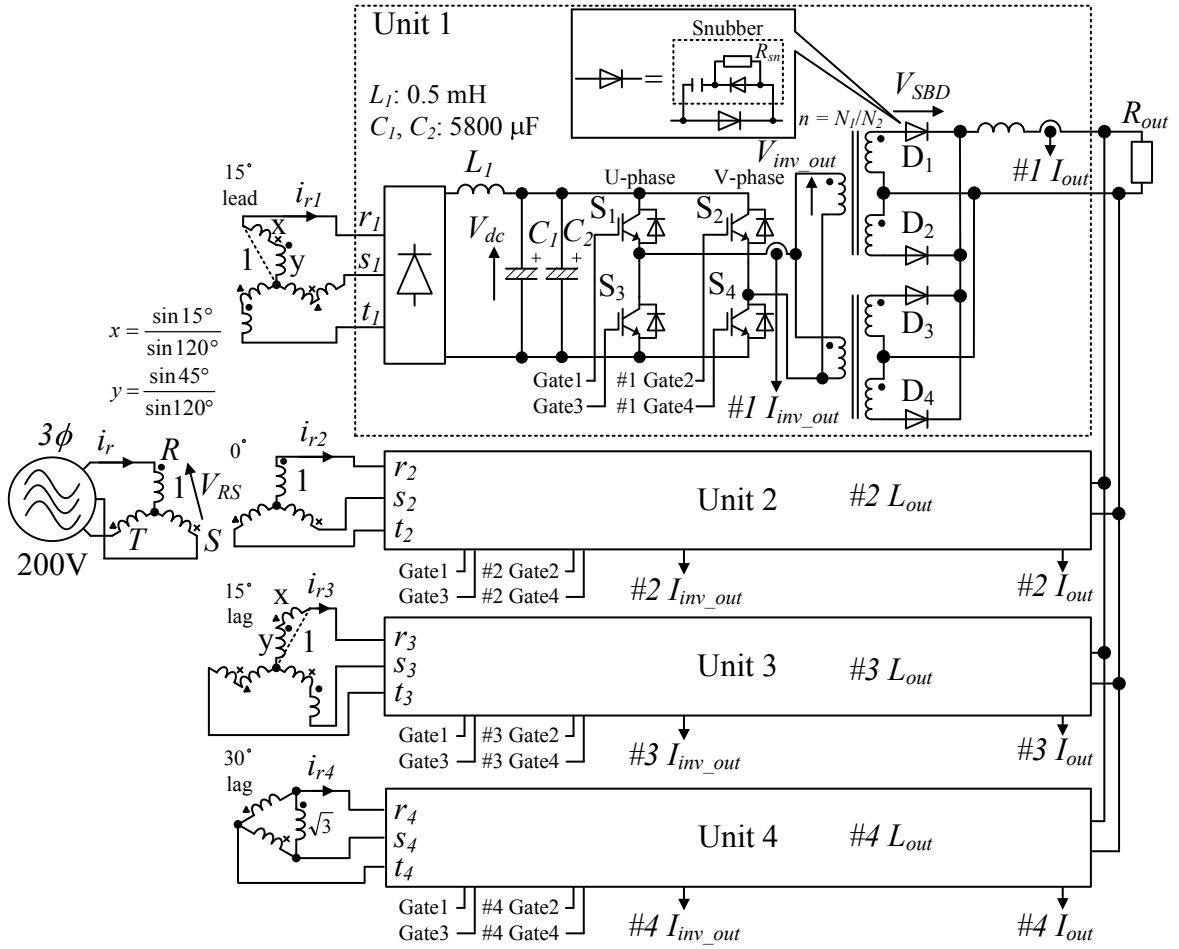

Fig. 1. Circuit configuration of the low-voltage, high-current circuit for sintering.

high frequency transformer, a snubber circuit and so on. Finally, it is clarified that experimental results of the surge voltage on the schottky barrier diode are correspond to the theoretical discussion by experiments.

II. Circuit Configuration of the Proposed System

A. Circuit Configuration

Fig. 1 shows the circuit configuration of the proposed system. This circuit can output 10,000 A due to the four 2,500 A units connected in parallel. Multiple transformers are connected to the input of the three-phase diode rectifier in order to reduce the harmonic components from the input grid current and also to improve the power factor of the grid. Moreover, snubber circuits are connected to schottky barrier diodes on the secondary side of the high frequency transformer in parallel in order to suppress the surge voltage after the commutation period [9, 10]. It is caused by wiring inductance including parasitic inductance of copper bus bar between the output terminal of the prototype circuit and an electric furnace, leakage inductance and parasitic capacitance of the schottky barrier diode. At next chapter, the snubber circuit is theoretically analyzed.

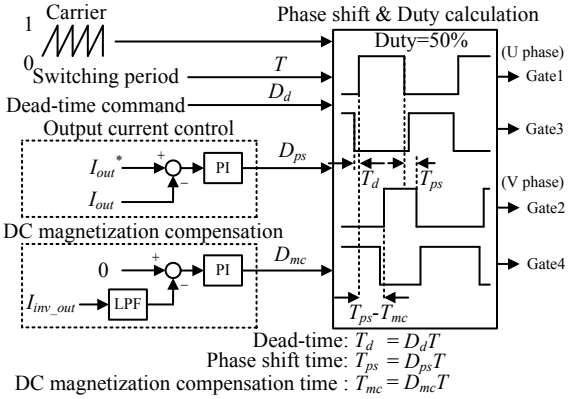

Fig. 2. Control diagram of the circuit.

B. Control Strategy

Fig. 2 shows a control diagram of the circuit. For each unit, the control strategy shown in Fig. 2 is independently implemented in order to guarantee that each unit output equal current. The gate signals of the U-phase are always operated with a 50% duty cycle. The gate signals of the V-phase are operated by phase shift control and duty control. When DC magnetizing occurs in the transformer due to the variability of the dead-time and the saturation voltage of the switch of the inverter, the duty cycle of the gate signals of

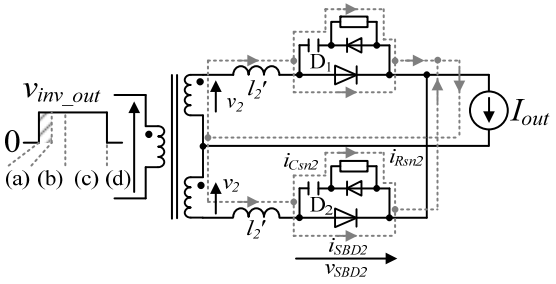

(a) Mode I

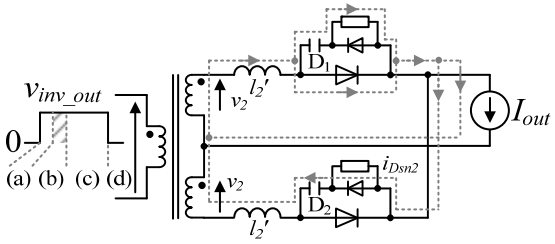

(b) Mode II

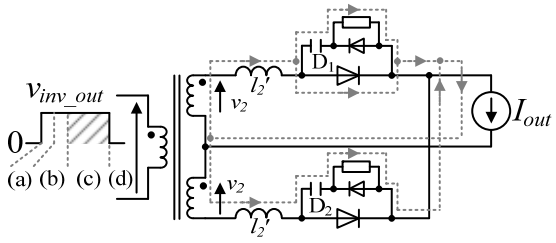

(c) Mode III

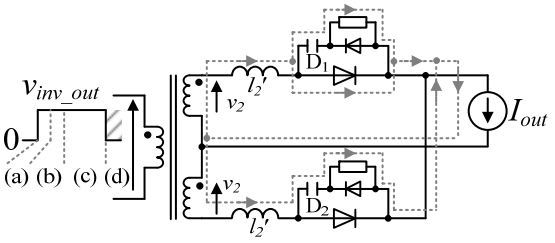

(d) Mode IV

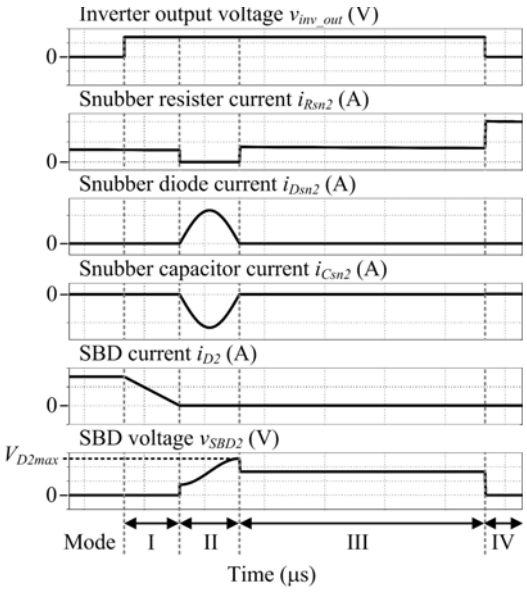

(e) Each simulation waveform

Fig. 3. Operation modes and ideal simulation waveforms.

the V-phase is controlled in order to suppress the dc component of the transformer current. The dc component of the transformer current is detected by the low-pass filter and compared to zero, which is the command of the DC component of the transformer current.

III. Snubber Circuit for Rectifier Circuit of Secondary Side of Transformer

In large output current applications, circuit components are connected in parallel. Actually, in the prototype circuit, schottky barrier diodes are connected in parallel on the secondary side of the transformer. Schottky barrier diodes feature no reverse recovery phenomenon which causes problems such as a short circuit between an upper switch and a lower switch, and surge voltage. However, due to parasitic capacitance of the diodes, the problem as mentioned above may occur even if the schottky barrier diode is used. Especially, when many devices are used, an equivalent parasitic capacitance is increased. Therefore, in large output current applications, parallel connection of rectifier diodes cause the surge voltage due to the parasitic capacitance. Therefore, proper design methods for the snubber circuits of schottky barrier diode on the secondary side of the transformer are needed. In this paper, a RCD snubber circuit which is connected to each schottky barrier diode is considered.

A. Suppression principle of the surge voltage

Fig. 3 shows the operation modes and ideal simulation waveforms when the surge voltage occurs on the schottky barrier diode D_2. In this paper, the RCD snubber which consists of a snubber resistor R_{sn}, a snuber capacitor C_{sn} and a snubber diode D_{sn}, is considered. It is noted that parasitic resistance, parasitic capacitance, parasitic inductance except the leakage inductance and forward voltage of the diodes are not considered for simplification of the principle of the RCD snubber circuit. In addition, a load is assumed as current source because the output resistance is dominant by parasitic inductance of copper bus bar.

Fig. 3(a) shows the mode I which is the commutation over lapping period. After the inverter output voltage is changed, both of diodes D_1 and D_2 are on-state. Therefore, the voltage of D_2 v_{SBD2} is almost zero. After Fig. 3 (a), the voltage of D_2 is increased as shown in Fig. 3 (e).

In the mode II (as shown in Fig. 3 (b)), the snubber capacitor is charged through the snubber diode. From Fig. 3 (b), the current of snubber capacitor $i_{Csn2}(t)$ is obtained by (1).

$$i_{Csn2}(t) = \frac{2v_2 - V_c(0)}{\sqrt{2l_2'/C_{sn}}} \sin\left(\frac{1}{\sqrt{2l_2'C_{sn}}}t\right) \quad (1)$$

where v_2 is the voltage of secondary side of the transformer, C_{sn} is the snubber capacitor, $V_c(0)$ is the initial voltage of the snubber capacitor, l_2' is the leakage inductance.

When the current of the snubber capacitor $i_{Csn2}(t)$ is reached to zero, the surge voltage of D_2 becomes maximum. From (1), the time t_1 which makes the current of the snubber capacitor zero is obtained by (2)

$$t_1 = \sqrt{2l_2'C_{sn}}\pi \quad (2)$$

Therefore, maximum voltage of D_2 when the RCD snuber is connected is expressed by (3) using the steady voltage $V_{D2steady}$ and the increment of the surge voltage $\Delta V_{D2surge}$

$$V_{D2\max} = \frac{1}{C_{sn}}\int_0^{t_1} i_{Csn2}(t)dt + V_c(0) = V_{D2steady} + \Delta V_{D2surge} \quad (3)$$

Here, $V_{D2steady}$ and $\Delta V_{D2surge}$ are expressed by (4).

$$\begin{cases} V_{D2steady} = 2V_2 \\ \Delta V_{D2surge} = 2V_2 - V_c(0) \end{cases} \quad (4)$$

After Fig. 3 (b), the snubber capacitor is discharged through the snubber resistor. In the mode III(as shown in Fig. 3 (c)), the snubber loss occurs.

In the mode IV (as shown in Fig. 3 (d)), D_2 is turned on according to the inverter output voltage. In the mode IV, the snubber loss also occurs.

B. Influence of parasitic capacitance of SBDs

In high current applications, many circuit components are connected in parallel. In Fig. 1, many SBDs on secondary side of the transformer are connected in parallel. As a result, an equivalent parasitic capacitance is increased. In this section, the influence of the parasitic capacitance of SBDs is investigated.

Fig. 4(a) shows the circuit diagram of the RCD snubber circuit with parasitic capacitance C_p. As shown in Fig. 4(a), the parasitic capacitance exists to the RCD snubber circuit in parallel.

Fig. 4(b) shows simulation waveforms of v_{SBD2} when the parasitic capacitance is not considered. In contrast, Fig. 4(c) shows simulation waveforms of v_{SBD2} when the parasitic capacitance is considered. Comparing Fig. 4(b) and (c), it is confirmed that the parasitic capacitance mainly affects to v_{SBD2} in the mode III. This is because the resonance occurs among the leakage inductance, the snubber capacitor and the parasitic capacitance when the snubber capacitance is discharged through the snubber resistor in the mode III. However, the maximum voltage of v_{SBD2} is not drastically changed because the snubber resistor works as a damping resistance. Therefore, it is confirmed that the parasitic capacitance does not drastically affect to the maximum voltage of v_{SBD2} by simulation.

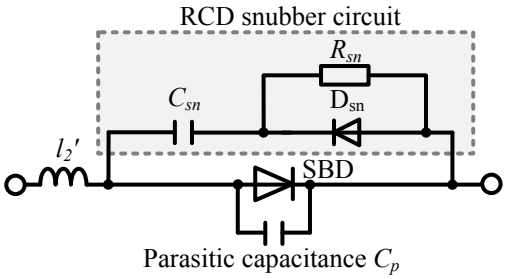

(a) RCD snubber circuit considering parasitic capacitance.

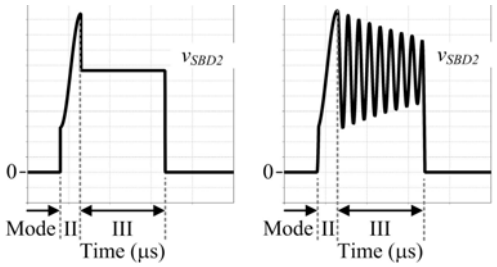

(b) Without parasitic capacitance. (c) With parasitic capacitance.

Fig. 4. Circuit diagram of RCD snubber circuit and simulation waveforms of v_{SBD2} considering parasitic capacitance.

C. Influence of parasitic inductance

Fig. 5 shows an equivalent circuit considering parasitic inductance in order to consider the influence of parasitic inductance when the snubber circuit cannot be closely connected to SBDs. L_R is a parasitic inductance of R_{sn}, L_D is a parasitic inductance of D_{sn}, and L_C is a parasitic inductance of C_{sn}. It is noted that the parasitic capacitance of SBD is also considered in this section.

In Fig. 5 (a), when the snubber capacitor is charged, the parasitic inductance of the snubber capacitor L_C and that of snubber diode L_D should be mainly considered. Both parasitic inductances contribute to vibration of the surge voltage as a resonance component with the snubber capacitor in the mode II. On the other hand, influence of the parasitic inductance of the snubber resistor does not affect in the mode II because the current does not flow to the snubber resistance.

On the other hand, In Fig. 5 (b), when the snubber capacitance is discharged, the parasitic inductance of the snubber capacitance L_C and that of the snubber resistance L_R should be taken into account. As mentioned in the section B of the chapter III, when the snubber capacitor is discharged, the resonance occurs among the leakage inductance, the snubber capacitor and the parasitic capacitance. Therefore, L_C and L_R affect the resonance. As a result, maximum current of the snubber resistor could be increased due to L_C and L_R.

Fig. 6 shows simulation results when each parasitic inductance is considered. From Fig. 6(a), it is confirmed that L_R does not affect in the mode II. On the other hand, from Fig. 6(b), it can be seen that L_D greatly affects to v_{SBD2}. As a result, the maximum value of v_{SBD2} could be increased. In addition, the snubber loss is also increased due to the vibration of the current of the snubber resistance because the snubber resistor works as the damping resistor. From Fig. 6(c), it is confirmed that the maximum value of v_{SBD2} could be increased by L_C. However, although the vibration of the current of the snubber resistance does not occur in the mode II, the maximum value of the current of the snubber resistor could be increased.

IV. Experimental Results

Fig. 7 shows the waveforms of the total output current and each output current when the square pulse of the current command which has 50 ms as on time and 50ms as off time is applied in a parallel operation of four units. Table I shows the experimental conditions. The total output current is calculated by adding each output current obtained as a comma-separated value (CSV) data. From Fig. 7, it is confirmed that each output current is not exactly square waveform because of inductances of copper bus bar between the output terminal of the prototype circuit and the electric furnace.

Fig. 8 shows temperature of each circuit components during the rated output current operation over three hours at constant ambient temperature of 26 degrees Celsius. It is noted that the output current is DC current in order to strictly test the prototype circuit in this experiment. In an actual SPS, high-current power supply should keep to output current for a few hours or a few days. From Fig. 8, the temperature of a snubber resistance is around 90 degrees Celsius, which is the highest in all devices. This temperature increase is due to the surge voltage of the schottky barrier diode. Temperature of the secondary winding of the high frequency transformer is around 80 degrees Celsius because of high output current. However, it is confirmed that the prototype circuit can achieve long continuous operation for sintering from the temperature experiment.

Fig. 9 shows waveforms of the inverter output voltage v_{inv_out}, the voltage of the schottky barrier diode v_{SBD2} and the current of the snubber resistor i_{Rsn}. From Fig. 9, it is confirmed that the surge voltage occurs on the schottky barrier diode after the commutation period as mentioned in the chapter III. It is noted that the capacitance and the resistance of the snubber circuit is not actually designed for low power loss in this experiment. However, it is experimentally confirmed that the oscillation of v_{SBD2} in the mode II and III corresponds to the theoretical discussion and the simulations.

V. Conclusion

In this paper, a prototype model was demonstrated with pulse output of 10,000 A in order to apply middle-large power for application in sintering. The prototype model consists of four units with output of 2,500 A in parallel. The

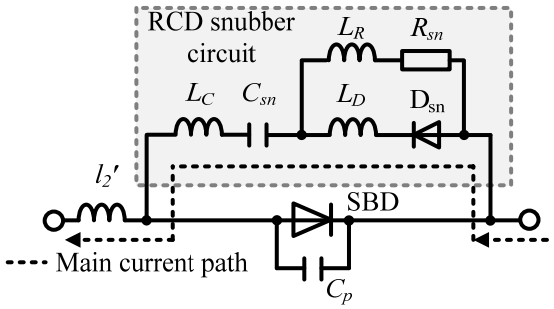

(a) When the snubber capacitor is charged in mode II.

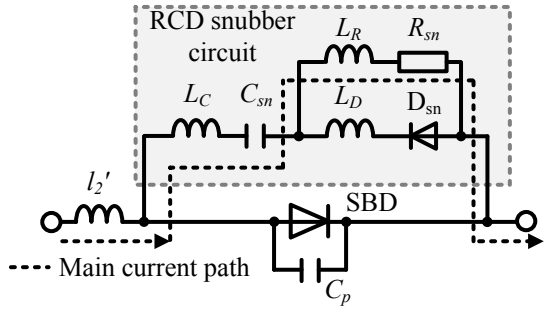

(b) When the snubber capacitor is discharged in mode III.

Fig. 5. Equivalent circuit of RCD snubber circuit including parasitic inductance.

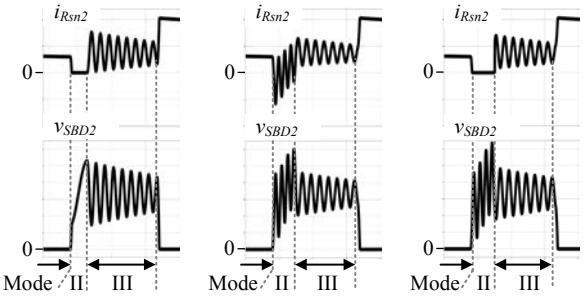

(a) L_R is considered. (b) L_D is considered. (c) L_C is considered.

Fig. 6. Simulation result when each parasitic inductance is considered (with parasitic capacitance of schottky barrier diode).

TABLE I. Experimental Conditions

Items	Value
Total output current I_{out}	10 (kA)
DC reactor L_1	0.5 (mH)
Smooth capacitor C_1, C_2	5800 (μF)
Switching frequency f_{sw}	15 (kHz)
Dead time T_d	4 (μs)
Turn ratio n	n=N_1/N_2=17

experimental results confirmed that the prototype circuit outputs pulse current of 7,200 A from the experiment of the long continuous operation. Moreover, from the temperature measurement, it was confirmed that the prototype circuit can achieve long continuous operation for sintering. Moreover, the influence of the parasitic capacitance of SBD, the influence of the parasitic inductance of each snubber component was theoretically discussed and simulated. Finally, it was experimentally confirmed that the voltage of SBD v_{SBD2} corresponds to the theoretical discussion and the simulations.

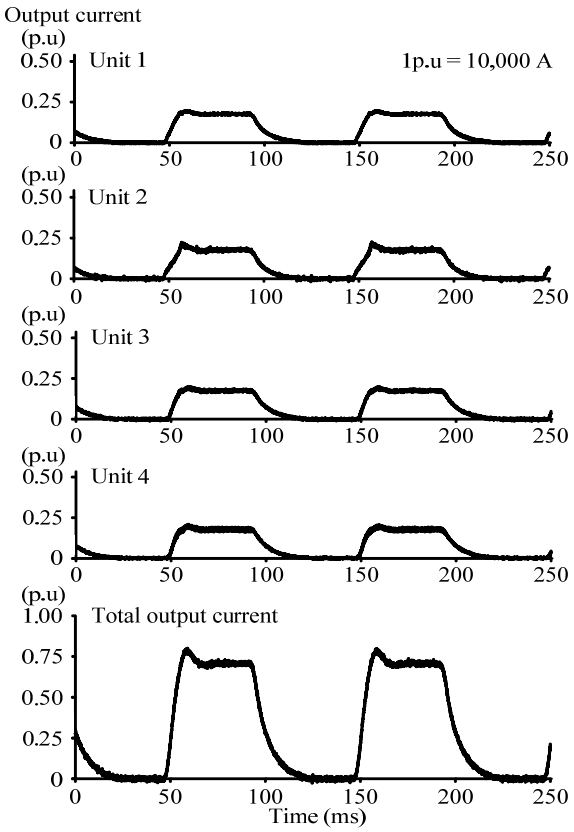

Fig. 7. Experimental output current waveforms.

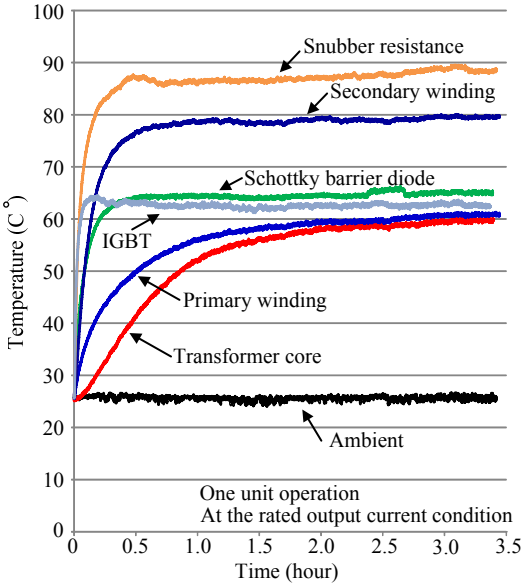

Fig. 8. Temperature of each circuit components during the rated current operation over three hours.

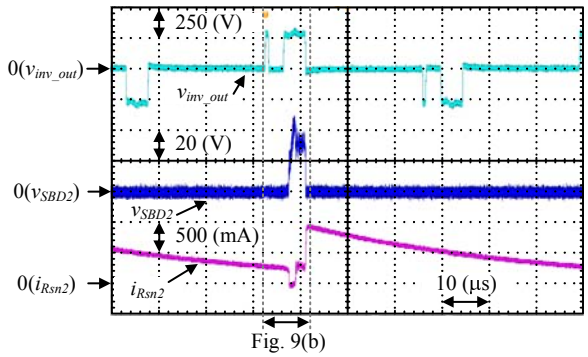

Fig. 9(b)

(a) Whole waveforms.

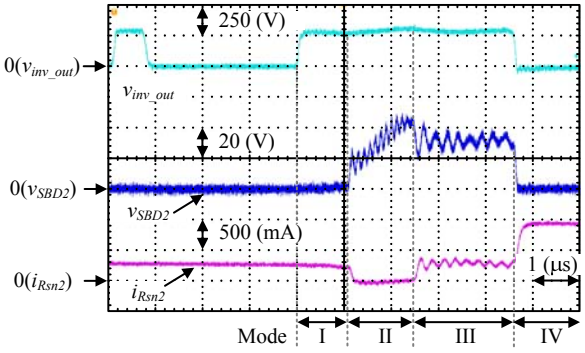

(b) Extended waveform.

Fig. 9. Experimental waveforms of SBD voltage and current of snubber resistor.

REFERENCES

[1] Galloway, James H. : "Power Factor and Load Characteristics for Thyristor Electrochemical Rectifier", IEEE transaction on Industrial Electronics, Vol. IA-13, No. 6, pp.607-611 (1977)

[2] J. R. Rodriguez, J. Pontt, C. Silva, E. P. Wiechmann, P. W. Hammond, F. W. Santucci, R. Alvarez, R. Musalem, S. Kouro, P. Lezana: "Large Current Rectifiers: State of the Art and Future Trends", Industrial Electronics, IEEE Transactions on , Vol.52, No.3, pp. 738-746 (2005)

[3] A. Siebert, A. Troedson, S. Ebner: "AC to DC Power Conversion Now and in the Future", Industrial Applications, IEEE Transactions on, Vol.38, No.4, pp. 934-940 (2005)

[4] P. Buddingh, J. R. St. Mars: "New Life for Old Thyristor Power Rectifiers Using Contemporary Digital Control", Industrial Applications, IEEE Transactions on, Vol.36, No.5, pp. 1449-1454 (2000)

[5] T. Noguchi, K. Nishiyama, Y. Asai and T. Matsubara : "Development of 13-V, 5000-A DC Power Supply with High-Frequency Transformer Coupling Applied to Electric Furnace", Power Electronics and Drives Systems, pp.1474-1479 (2005)

[6] R. Nakanishi, T. Noguchi, I. Takahashi and M.Tanaka : "Development of Low-Voltage and High-Current DC Power Supply Featured Small-Size and High-efficiency", SPC-00-61, pp.37 (2000) (in Japanese)

[7] K. Ishida and T. Noguchi : "Development of Low-Voltage and Large-Current DC Power Supply with High-Frequency Transformer Coupling", Proceedings of IEEJ Industry Applications Society Annual Conference, Vol.1, pp.493 (2003) (in Japanese)

[8] K. Orikawa, J. Itoh: "Power Loss Reduction of a AC-DC Converter Features 10-V and 10000-A for Sintering Power Supply", EPE-PEMC 2012, LS3e (ISS-12) (2012)

[9] K. Orikawa, J. Itoh: "Analysis and Optimization Design of Snubber Circuit for Isolated DC-DC Converters in DC Power Grid", ICRERA (2012)

[10] K. Domoto, Y. Ishizuka, S. Abe, T. Ninomiya: "Control Characteristics Improvement of Full-Bridge DC-DC Converter with Snubber Capacitor ", The 2014 International Power Electronics Conference, No. 21A4-4, pp. 3652-3658 (2014)